remote sensing

MDPI

Article

# Exploring Relationships among Tree-Ring Growth, Climate Variability, and Seasonal Leaf Activity on Varying Timescales and Spatial Resolutions

**Upasana Bhuyan [1,*], Christian Zang [2], Sergio M. Vicente-Serrano [3] and Annette Menzel [1,4]**

1 Ecoclimatology, Department of Ecology and Ecosystem Management, Technische Universität München, Freising 85354, Germany; amenzel@wzw.tum.de
2 Land Surface-Atmosphere Interactions, Department of Ecology and Ecosystem Management, Technische Universität München, Freising 85354, Germany; christian.zang@wzw.tum.de
3 Instituto Pirenaico de Ecología, Consejo Superior de Investigaciones Científicas (IPE–CSIC), Zaragoza 50059, Spain; svicen@ipe.csic.es
4 Institute for Advanced Study, Technische Universität München, Garching 85748, Germany
* Correspondence: bhuyan@wzw.tum.de; Tel.: +49(0)8161-714-746

Academic Editors: John S. Kimball, Kaiyu Guan, Lars T. Waser and Prasad S. Thenkabail
Received: 22 February 2017; Accepted: 22 May 2017; Published: 25 May 2017

**Abstract:** In the first section of this study, we explored the relationship between ring width index (RWI) and normalized difference vegetation index (NDVI) time series on varying timescales and spatial resolutions, hypothesizing positive associations between RWI and current and previous- year NDVI at 69 forest sites scattered in the Northern Hemisphere. We noted that the relationship between RWI and NDVI varies over space and between tree types (deciduous versus coniferous), bioclimatic zones, cumulative NDVI periods, and spatial resolutions. The high-spatial-resolution NDVI (MODIS) reflected stronger growth patterns than those with coarse-spatial-resolution NDVI (GIMMS3g). In the second section, we explore the link between RWI, climate and NDVI phenological metrics (in place of NDVI) for the same forest sites using random forest models to assess the complicated and nonlinear relationships among them. The results are as following (a) The model using high-spatial-resolution NDVI time series explained a higher proportion of the variance in RWI than that of the model using coarse-spatial-resolution NDVI time series. (b) Amongst all NDVI phenological metrics, summer NDVI sum could best explain RWI followed by the previous year's summer NDVI sum and the previous year's spring NDVI sum. (c) We demonstrated the potential of NDVI metrics derived from phenology to improve the existing RWI-climate relationships. However, further research is required to investigate the robustness of the relationship between NDVI and RWI, particularly when more tree-ring data and longer records of the high-spatial-resolution NDVI become available.

**Keywords:** radial growth; NDVI; MODIS; GIMMS3g; phenology; dendroecology; scPDSI

## 1. Introduction

Remote sensing and dendroecology are considered instrumental in monitoring net primary productivity [1,2]. Dendroecologists have successfully used samples of tree growth from radial increments to quantify long-term variability in forest productivity [3,4]. Tree-ring width or annual radial growth increment is a widely used proxy for tree vitality [5], and its connections to climate and extreme climatic events, such as drought, are well established [5,6]. However, preparing tree-ring chronologies involves time-consuming field and laboratory work, thereby undermining the technique's potential to be used for monitoring real-time forest growth over large spatial scales [7–9]. Real-time observations based on remote sensing are also not feasible; however, at the end of the growing season, a solid assessment of the past annual growth should be possible. The remotely

sensed normalized difference vegetation index (NDVI), which is based on red and near-infrared reflectances [10], is a good measure of photosynthetic activity at landscape-scales and can be used to estimate vegetation productivity [1,11–17]. Against the background of global climate warming and an associated lengthening of the growing season [18,19], studying how climatic factors and NDVI are related to ring width index (RWI) could lead to a better and more immediate understanding of forest growth.

The utility of remote sensing indices in observing and monitoring phenology over large scales and at regular intervals has been well documented [20], and a handful of studies have related NDVI directly to tree-rings [4,7,12–15,21,22]. Although these studies linked NDVI values with tree-ring growth data, the relationship of the latter with NDVI phenological metrics remains to be explored. From an ecological perspective, plant phenology plays a significant role in determining the carbon sequestration period of terrestrial ecosystems and is widely used to diagnose responses of ecosystems to global change [23–25]. Accurate information related to phenology is important in the study of regional-to-global carbon budgets [26]; hence, exploring its role in explaining tree-ring growth could be crucial.

Remote sensing of phenology using time series of vegetation indices is based on the intra-annual changes of canopy greenness [25]. We have extracted important phenological metrics from NDVI time series to examine their relationship with RWI because the spatio-temporal variations of vegetation phenology are known to serve as important indicators of photosynthetic activity [27]. We analyzed NDVI time series to extract key phenological metrics, such as the start of the growing season (SOS) and end of the growing season (EOS). These characteristics may not necessarily correspond directly to defined, ground-based phenological events, but they do provide indications of seasonal ecosystem dynamics [25]. They can reveal landscape-scale climate/tree-ring growth interactions. We compared RWI time-series from 69 forest sites with NDVI at fine (250 m, MODIS) and coarse (8 km, GIMMS3g) spatial resolutions for different timescales (cumulative NDVI values from one to 20 observations). Tree-ring width as a proxy for tree growth is known to correlate with several monthly values of temperature and precipitation during the year of growth and, in some cases, previous years (e.g., [5,28]). Intercomparison of corresponding data of tree-ring growth, climate, and NDVI may help deepen our understanding of the response of a forest to recent warming trends.

In the first section of this study, we evaluated whether NDVI correlates with the radial growth of trees scattered in the Northern Hemisphere. In the second section, we tried to fill the gap in literature that exists in exploring the relationship between RWI and various NDVI phenological metrics. Overall, we seek to resolve whether NDVI metrics can help to refine or improve the existing RWI-climate relationship, and whether such metrics could be used for explaining the RWI. If so, such knowledge could be useful in supporting forest management practices.

## 2. Materials and Methods

### *2.1. NDVI Data*

We used two NDVI datasets with different spatial resolutions: (1) Moderate Resolution Imaging Spectroradiometer (MODIS) and (2) Global Inventory Modeling and Mapping Studies 3g (GIMMS3g). This allowed us to study the possible effects of spatial resolution on the RWI-NDVI relationship. For MODIS, we used MOD13Q1 [29], which is the MODIS/Terra vegetation index. It has a spatial resolution of 250 m and is provided as a 16-day composite, resulting in 23 observations per year. Quality information was used to discard possible snow and cloud values. The MODIS NDVI record begins in February 2000; however, we analyzed data from 2001 (the first complete year of NDVI data) until 2010, the last year of our assembled tree-ring dataset.

The third-generation Global Inventory Modeling and Mapping Studies, GIMMS3g [30] is based on the Advanced Very High Resolution Radiometer (AVHRR), has a spatial resolution of 8 km, and is provided at a temporal resolution of 15 days resulting in two maximum-value composites per month and 24 observations per year. The GIMMS3g NDVI record begins in July 1981; we analyzed data

from 1982 (the first complete year of NDVI data) to the end of 2010 to maximize the overlap with the assembled tree-ring dataset. The latitude and longitude of each of the tree-ring sites were used to select the corresponding pixel from the GIMMS3g and MODIS NDVI datasets. For each annual NDVI time series, cumulative values (1–20 observations) were calculated and then used in the Pearson correlation analysis. For instance, a cumulative NDVI value of five implies that the data from the current observation and of four previous observations (four observations equates to approximately two months) will be used to compute the cumulative NDVI value (sum) for a given time.

### 2.2. Tree-ring Data

Tree-ring data were downloaded from the International Tree-Ring Data Bank (ITRDB) [31] which is a repository containing tree-ring data [32]. All downloaded time series from the ITRDB were filtered for three requirements (1) tree-ring widths complete for the period 1982 to 2010, (2) no missing NDVI data in the time-series of each overlapping pixel, and (3) having forest cover in the corresponding remote sensing pixel. For the third requirement, we used the world forest-cover map GlobCover from the European Space Agency, which is based on Envisat Medium Resolution Imaging Spectrometer (MERIS) data between December 2004 and June 2006 [33]. We excluded tree-ring sites in remote sensing pixels covering bare areas, water bodies, areas with permanent snow and ice, or areas located in the Southern Hemisphere. In total, 69 sites were retained for the analysis (Figure 1). Each tree-ring series was detrended on a per-site basis using a cubic-smoothing spline with a frequency response of 50% at 32 years [34]. This was done to remove the trend present in the original raw tree-ring width measurements, while at the same time preserving the inter-annual to decadal variability. Prior to detrending, the series were power-transformed to remove temporal heteroscedasticity, and were then robustly averaged into dimensionless chronologies of RWIs. Readers unfamiliar with tree-ring detrending and chronology development can refer to Cook et al. [9]. Table S1 (Supplementary) gives all information on sites, species, climate zones (see Section 2.3), chronology coverage, and important tree-ring metrics.

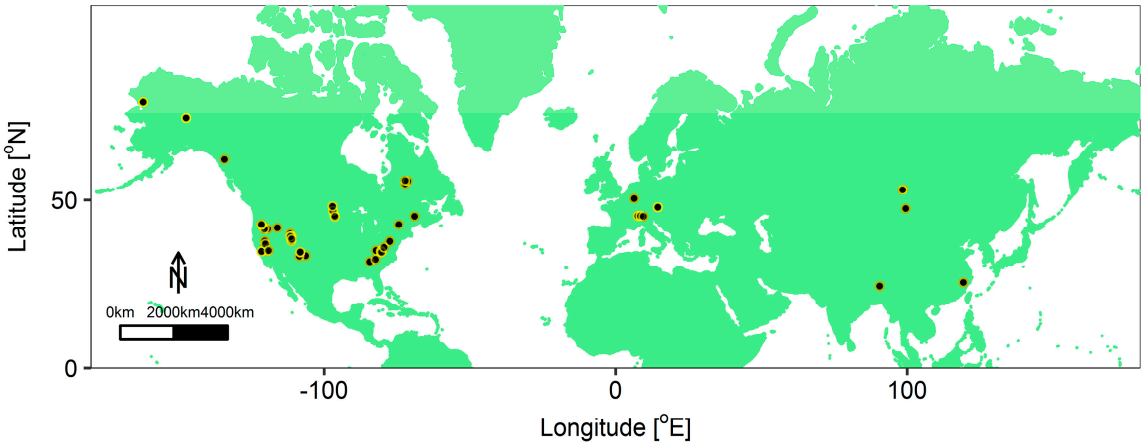


**Figure 1.** World map showing the location of the 69 study sites.

### 2.3. Climate Data

We used monthly mean temperature (TMP), mean monthly sums of precipitation (PRE), and potential evapotranspiration (PET) from the CRU TS 3.21 dataset [35] available on a 0.5° grid [36]. Monthly time series of the self-calibrating Palmer Drought Severity Index (scPDSI) [37] on a 0.5° grid were downloaded from the KNMI Climate Explorer web page [38]. The drought index Standardized Precipitation Evapotranspiration Index (SPEI) was calculated using the R package SPEI [39] based on input data from CRU. Climate was classified according to the world Köppen–Geiger climate-classification map [40], in which zone B indicates an arid/semiarid climate, C and D are temperate and continental climates, respectively. Conifer sites were analyzed separately for the three climate zones (B, C, and D) (4, 21, and 28 sites, respectively), whereas the 16 sites with broadleaf forests constituted the fourth group (see Table S1).

### 2.4. Extracting Phenological Metrics from the NDVI Time Series

Annual time series of NDVI allow the extraction of key phenological events such as the start (SOS) and end (EOS) of the growing season as well as of different NDVI metrics. However, prior to this, the NDVI time series had to be preprocessed to deal with perturbations due to atmospheric and geometric interferences and noise.

In the case of MODIS, individual NDVI observations that were marked in the corresponding pixel-reliability layer as either missing or as affected by snow or clouds were removed. Only those marked as good were retained in the NDVI time series that, despite containing gaps, constituted reliable and uncontaminated data; the gaps were then linearly interpolated. In the case of GIMMS3g, it was not necessary to discard data based on a quality layer because the GIMMS3g data had already been corrected for solar zenith and viewing angles, volcanic aerosols, atmospheric water vapor, and cloud cover [41], thus assuring the quality and consistency of the data.

To extract the seasonality of the NDVI time series, the series were filtered using a Gaussian filter [42] to remove noise. As mentioned in Misra et al. [43], the weights in the Gaussian filter were distributed symmetrically around the central value, and their fractional weights *Wi* were calculated as follows:

$$W_i = \frac{1}{0.5 * k * \sqrt{pi}} * \exp * \left(-\frac{w_i^2}{(0.5 * k)^2}\right), \quad (1)$$

where k is the size of the filter and $w_i$ is the $i$th value in a sequence from $-k$ to k; for this study, we used k = 6. To achieve values that summed to unity, $W_i$ was normalized by the sum of itself. Deviations of the raw NDVI from the Gaussian-filtered data were z-transformed, and values beyond two standard deviations were considered outliers and removed from the raw data. After removing such outliers, the NDVI data were again smoothed using the weighted Gaussian filter and then linearly interpolated to daily values.

Based on these daily NDVI time series, a threshold of 50% of the seasonal amplitude was used to define the start (SOS) and end (EOS) of the growing season. An example of a processed NDVI time series with the phenological parameters SOS and EOS is given in Figure S1 (Supplementary). For subsequent use in the modelling approach, we calculated ten different NDVI phenological metrics (Table 1), that we then standardized using the site-specific mean and standard deviation. These NDVI metrics derived from phenology are subsequently referred to as NDVI phenological metrics.

**Table 1.** Phenological metrics calculated from normalized difference vegetation index (NDVI) time series.

| Phenological Metric | Definition |
|---|---|
| NDVI_GS | sum of the NDVI values extracted from the start of season to the end of season |
| NDVI_GS_prv | sum of the NDVI values extracted from the start of season to the end of season of previous year |
| NDVI_Sum | sum of the NDVI values of the summer months June to August |
| NDVI_Sum_prv | sum of the NDVI values of the summer months of previous year |
| NDVI_Spr | sum of the NDVI values of the spring months March to May |
| NDVI_Spr_prv | sum of the NDVI values of the spring months of previous year |
| NDVI_SOS | NDVI extracted at the start of season |
| NDVI_SOS_prv | NDVI extracted at the start of season of the previous year |
| SOS_date | date of the start of season |
| EOS_date_prv | date of the end of season of the previous year |

### *2.5. Statistical Analyses*

In order to assess the relationships between tree growth and NDVI, Pearson correlations between RWI and cumulative NDVI (MODIS and GIMMS3g) for the 69 study sites were calculated for different timescales of NDVI integration. The resulting correlation coefficients were summarized for both MODIS and GIMMS3g, as well as for the four climate groups (deciduous of all climate zones, coniferous in climate zone B, in C, and in D) by calculating the mean and variance of each group.

### *2.6. Relationship of RWI with NDVI Metrics and Climate*

To establish quantitative relationships between ground-based RWI, climate, and phenological metrics derived from NDVI time series, we performed random forest (RF) analysis as a multivariate non-parametric regression method [44–47]. The RF model, which is an ensemble learning technique developed by Breiman [45], was fitted using all tree-ring sites. We used 70% of the data randomly sampled to train the RF and the remaining were retained for RF prediction-error testing. The proportion of explained variance in the outcome of the training data and the normalized root mean square error (NRMSE) were used to quantify the association between RWI and NDVI / climate. The normalized root mean square error (NRMSE) is computed as NRMSE = sqrt $(n^{-1}\sum_{1}^{n}\{x_{obs} - x_{model}\}^2))/n^{-1}\sum_{1}^{n}x_{obs}$ = RMSE/mean$(x_{obs})$, where $x_{obs}$ and $x_{model}$ refer to observed RWI values (of the test data) and predicted RWI values of the RF model respectively. The variance explained is computed as $(1 - \text{MSE}/\text{var}(x_{obs}))$ of the training data. To evaluate the importance of predictors, we used the Increased Mean Square Error which is a robust measure defined as the increase in the mean squared error of predictions as a result of the variable being permuted. Higher values indicate a variable that is more important [45]. A second measure for variable importance, the Increased Impurity Index, relates to the loss function by which best splits are chosen. More important variables achieve higher increases in node purities. RF analysis was performed in the R statistical environment [48] using the randomForest package [49].

To assess the importance of NDVI phenological metrics derived from two different remote sensing products, we fixed the period of analysis from 2001 to 2010 in order to have a fair comparison using the same time span for the models. In this way, we had an identical RWI-climate model, to which NDVI phenological metrics from both MODIS and GIMMS3g were added. In the RWI-climate model, RWI was explained by predictors: scPDSI (self-calibrating Palmer Drought Severity Index), PRE (monthly sums of precipitation), TMP (monthly mean temperature), latitude of the forest site, elevation of the forest site, tree type (coniferous or broadleaf), and climate zone (B, C, or D) as per Köppen–Geiger climate classification. To explain tree growth (RWI) by MODIS/GIMMS3g NDVI and climate, the number of regression trees in RF was fixed to 200, and the number of variables sampled at each node was set to seven after a preliminary analysis. For the RF climate-NDVI models, besides the predictors of the RWI-climate model, 10 standardized NDVI phenological metrics, namely NDVI_GS, NDVI_GS_prv, NDVI_Sum, NDVI_Sum_prv, NDVI_Spr, NDVI_Spr_prv, NDVI_SOS, NDVI_SOS_prv, SOS_date, and EOS_date_prv (see Table 1) were used. The same analysis was also performed with

drought index SPEI (Figure S5, Supplementary), however, it is not presented in the manuscript as it explained less variance of the RWI in comparison to drought index scPDSI. We performed a validation of the RF model (MODIS) using a test dataset corresponding to 30% of the original dataset randomly sampled. We report here the mean relative error (RE), ratio of root mean square error (RMSE), and ratio of mean absolute error (MAE) as validation statistics. The formulas used to calculate these metrics are given in Section S3 (Supplementary). Additionally, we provide the scatterplot between observed RWI values from the test dataset and predicted RWI values from the RF model (Figure S4, Supplementary).

## 3. Results

### *3.1. Relationships between RWI and NDVI/Climate*

A typical pattern of Pearson correlation coefficients between annual RWI and cumulative NDVI (up to 20 observations) is given in Figure 2 for a site in Utah (UT531), United States of America, with a continental-type (D) climate and a RWI series for tree species *Juniperus scopulorum* Sarg. The correlation patterns based on GIMMS3g NDVI (8 km resolution, 29 years of data) and MODIS NDVI (250 m resolution, 10 years of data) for up to 20 cumulative observations are quite similar. The NDVI from May–June (observations 10+) until August–September (observations 15+) and integrating up to 15 cumulative time points show positive associations with the corresponding annual RWI. However, the correlation based on the MODIS resolution and time frame is stronger and sharper in time compared to the respective GIMMS3g ones, pointing to May–September (observations 15+) as the decisive months for forest growth.

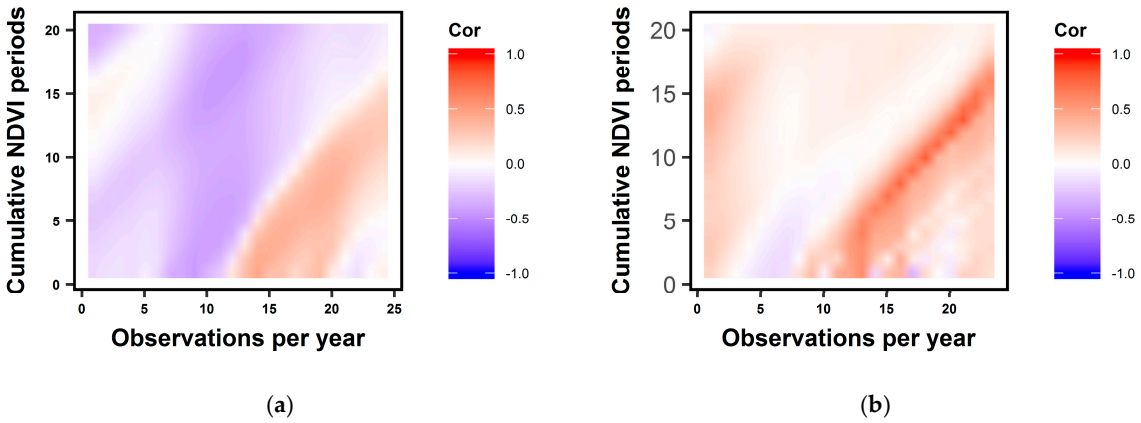


**Figure 2.** Pearson correlation coefficients between time series of ring width index (RWI) and cumulative NDVI at different temporal scales (1–20, y-axis) at a continental D climate site with a coniferous forest in Utah, United States of America for (**a**) GIMMS3g, 8 km resolution (1982–2010) with 24 time points in a year (x-axis) and (**b**) MODIS, 250 m resolution (2001–2010) with 23 time points in a year (x-axis).

In general, the correlation patterns between RWI and NDVI show these positive inter-annual associations, yet strong variations with species type (deciduous versus coniferous), climatic zone (B, C, and D), spatial scale (GIMMS3g versus MODIS), and integration time (up to 20 observations of the NDVI time series) are observed. Figure 3 displays the correlation patterns for all sites summarized as mean correlations of the four groups. For broadleaf species, growth in terms of RWI is (if at all) represented by MODIS NDVI during spring and the optimal length of the cumulative time period is not well defined. The signal for GIMMS3g NDVI is even weaker, more spread-out, and does not display any pattern. For coniferous trees in the semiarid to arid climate zone B, tree growth is strongly associated with a wide-ranging MODIS NDVI signal, from the start of the year until early summer and for cumulative periods of up to 15–20 NDVI observations. For GIMMS3g NDVI, RWI is tightly linked to NDVI of summer months and up to 20 cumulative NDVI observations. For conifers in

climate zone C, the MODIS NDVI growth signal is stronger than the GIMMS3g NDVI signal. It is represented by summer months at a cumulative period of up to 7–10 NDVI observations, whereas the weaker GIMMS3g signal has cumulative periods of up to 15–20 NDVI observations. For conifers in climate zone D, the MODIS NDVI signal is strong and represents growth during the summer and up to 10–15 cumulative NDVI observations. In contrast, the GIMMS3g NDVI signal is almost nonexistent. The corresponding variances of the respective Pearson correlation coefficients are shown in Figure S2 (Supplementary).

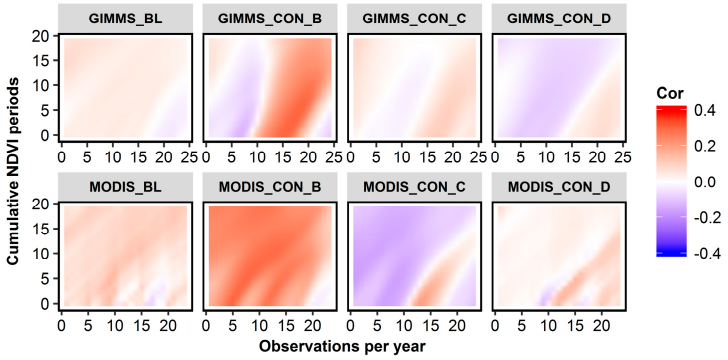


**Figure 3.** Mean Pearson correlation coefficients between time series of RWI and cumulative NDVI at different temporal scales (1–20, y-axis) for 69 tree-ring sites. Cumulative NDVI is either based on GIMMS3g (8 km resolution, 1982–2010) or MODIS (250 m resolution, 2000–2010). BL indicates 16 sites with broadleaf species, CON_B, CON_C, and CON_D refers to 4, 21, and 28 sites with coniferous tree species in climate zones B, C, and D, respectively. BL and CON refer to broadleaf and conifer species respectively. Zone B indicates arid/semiarid climate, C and D represent temperate and continental climates, respectively, as per the Köppen—Geiger climate classification [40].

### *3.2. Explaining RWI with NDVI Metrics and Climate*

#### 3.2.1. Variable Importance in RF based on MODIS NDVI/Climate

The RWI-climate model explained 28.2% of the variance of the RWI. When MODIS NDVI predictors were added to the model, the RWI-climate-NDVI model (Table 2) explained 37.2% of the variance of the RWI. The results of the RFs to describe the relationship between RWI and conditioning factors (MODIS NDVI /climate) in terms of the importance of the selected variables are shown in Figure 4. The Increased Mean Square Error lists the seven most important variables as scPDSI (9.30), NDVI_Sum (4.66), NDVI_Spr_prv (3.00), PRE (2.82), NDVI_Sum_prv (2.27), Latitude (2.24) and NDVI_GS (1.88). We notice similar results according to the Increased Impurity Index, which lists scPDSI (1.40), NDVI_Sum (0.61), PRE (0.42), NDVI_Sum_prv (0.27), NDVI_Spr_prv (0.24), Latitude (0.23), and NDVI_Spr (0.23) as the most important variables for the model.

**Table 2.** Results of RF models to explain RWI using two different datasets (GIMMS3g and MODIS). Here, NRMSE denotes the normalized root mean square error (in test data), and the explained variance is the explained-variation proportion in the outcome of the training data. The period of analysis for both the RF models is 2001 to 2010.

| Model No. | Response Variable | Dataset | Explained Variance | Important Predictor Variables | NRMSE |
|---|---|---|---|---|---|
| 1 | RWI | Climate + MODIS NDVI | 37.2% | scPDSI, NDVI_Sum, NDVI_Spr_prv, PRE, NDVI_Sum_prv, Latitude NDVI_GS | 0.13 |
| 2 | RWI | Climate + GIMMS3g NDVI | 29.7% | scPDSI, NDVI_Sum, TMP, NDVI_Sum_prv, Elevation, NDVI_GS_prv, Latitude | 0.26 |

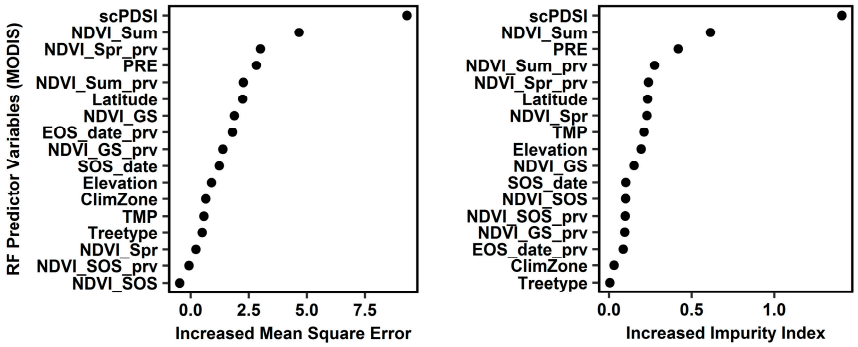


**Figure 4.** Random-forest variable-importance plot for RF (MODIS) climate-NDVI model. Variables are ranked in terms of importance on the y-axis (with variables of highest importance for explaining RWI at the top). PRE, TMP, scPDSI, Latitude, Elevation, Tree type, and ClimZone represent precipitation, temperature, self-calibrating Palmer Drought Severity Index, latitude of the forest site, elevation of the forest site, tree type (coniferous or broadleaf), and climate zone (B, C or D) as per the Köppen–Geiger climate classification [40], respectively. For definitions of the NDVI phenological metrics: NDVI_GS, NDVI_GS_prv, NDVI_Sum, NDVI_Sum_prv, NDVI_Spr, NDVI_Spr_prv, NDVI_SOS, NDVI_SOS_prv, SOS_date, and EOS_date_prv, see Table 1.

#### 3.2.2. Variable Importance in RF based on GIMMS3g NDVI/Climate

An analogous RF approach was used to model tree growth with climate and GIMMS3g NDVI. The RWI-climate model explained 28.2% of the variance of the RWI. When GIMMS3g NDVI predictors were added to the RWI-climate model, the RWI-climate-NDVI model (Table 2) explained 29.7% of the variance. In general, the importance of predictors was found to be similar to the case of MODIS NDVI, however, the model explained less variance compared to the model with MODIS data. The variable-importance measure, the Increased Mean Square Error lists scPDSI, NDVI_Sum, TMP, NDVI_Sum_prv, Elevation, NDVI_GS_prv and Latitude as the most important variables. The Increased Impurity Index lists NDVI_Spr, scPDSI, Latitude, NDVI_GS, PRE, NDVI_GS_prv, and NDVI_Sum as the important variables. As the increase in variance explained after adding NDVI metrics was approximately 1.5%, the results of the GIMMS3g NDVI are not discussed in detail.

### *3.3. Important NDVI Metrics and Validation of MODIS RF Model*

We extracted several phenological parameters from the NDVI time series. However, it was shown that not all of the extracted parameters were equally important for the RF models. When added to climate, the following NDVI phenological metrics better explained tree-ring growth: Summer NDVI of the current and previous year followed by spring NDVI of the previous year and growing season NDVI of current and previous year. While validating the model, the following validation metrics were computed: the mean RE (0.03), the MAE ratio (0.66) and the RMSE ratio (0.53). The ratios which were calculated between the values of the RF model and the test dataset showed weak prediction skills of the validation model and in general performed approximately half as well as the RF model. A scatterplot between the observed RWI from the test dataset and predicted RWI from the RF model, (Figure S4, Supplementary) show that they are not very well correlated.

## 4. Discussion

### *4.1. Relationship between RWI-NDVI*

In general, a positive relationship between NDVI in the growing season and RWI was seen for many forests in our study. Early work by Kaufmann et al. [50] based on GIMMS data equally showed a positive correlation between tree-rings and NDVI over the entire growing season and monthly values for April–July and October. Nevertheless, the positive and robust relationship observed between radial

growth and NDVI identified for 69 sites across the Northern Hemisphere at the local level cannot be considered a rule on the global scale [7]. For broadleaf species of different climate zones (B, C, D), we found that growth in terms of RWI was only weakly correlated by a weak MODIS NDVI signal during spring, with the optimal length of the cumulative time period not well defined and by an even weaker GIMMS3g signal that did not display any clear pattern. This is in line with findings of Brehaut et al. [51] for Northern Canada, where little or no correlation across the region for deciduous trees was observed. For conifers in a continental (D) climate, growth was linked to a MODIS NDVI signal during summer at cumulative NDVI periods of up to 10–15. This finding is supported by earlier studies based on GIMMS data, e.g. by Lopatin et al. [14] for continental Russia reporting a similar positive association between NDVI of June to August and conifer growth (Siberian spruce and Scots pine) as well as by Bunn et al. [4] for Siberia. Similarly, for North America, studies have reported positive associations between NDVI and conifer ring-widths for the interior of Alaska [52], for Siberia/Canada [22], and for Northern Canada [51]. However, this is contradictory to a study by Beck et al. [21], who found no significant correlation between ring-widths of Canadian spruce and NDVI at any point during the growing season. It should be pointed out here that the majority of the studies mentioned above used GIMMS/GIMMS3g NDVI for their analyses and not MODIS as in our study. For conifers in semiarid (B) climate, growth was represented by a wide-ranging MODIS NDVI signal but this was tightly linked to summer months at a cumulative period of up to 20 by GIMMS3g. For conifers in a temperate (C) climate, growth was strongly represented by MODIS NDVI of summer months at a cumulative period of up to 10. There are no comparable studies for these climate regions to support or contradict our findings. The variance of the Pearson correlation coefficients between NDVI and RWI was generally small (see Supplementary, Figure S2) except for conifer species in arid/semi-arid zone B, indicating that there is some confidence in the above interpretation. The comparably large variance in the correlation coefficient for the B climate zone is most likely due to the small number of sites (n = 4) included. In some forests in our study, a negative relationship between NDVI and RWI was observed. The reasons for such a mismatch could be varied growth-responses of trees depending on site-level factors [53], or the effects of changing environmental conditions.

### *4.2. Relationship between RWI, NDVI Phenological Metrics and Climate Parameters Based on RF Model*

In general, when comparing the variables identified as important in the RF approach, it should be noted that the variable-importance score depends on the number of included variables. Removing or replacing predictors, for example, may change the importance scores because different inter-correlated variables could act as surrogates. RFs use bagging to build the many different decision trees on the same dataset. While each individual decision would fit the identical model to the exact same data, a different aggregate model is observed each run because it takes different bootstrap samples. Nevertheless, in the second part of this study (Section 3.2), we could demonstrate that NDVI phenological metrics have the potential to improve relationships between RWI and climate. In order to identify the most important NDVI metrics derived from phenology, we ran various random forest models to explain RWI of the period 2001–2010; firstly using climate data as predictors and secondly using both climate and NDVI metrics as predictors. Using MODIS NDVI metrics and climate data, 37.2% of the variance of RWI could be explained, increasing it from 28.2% if only climate was used as predictor for RWI (see Table 2). In contrast, for the GIMMS3g model, the increase was approximately 1.5 percent (28.2% versus 29.7%) after adding NDVI metrics. This clearly underlines that including MODIS NDVI based phenological information improved the RWI modelling noticeably. The difference in performance of the two NDVI based models could be because high-spatial-resolution of the MODIS data is able to capture local climatic or other information reflecting the changes in vegetation or RWI better than the coarse-spatial-resolution GIMMS data, since the latter with a spatial-resolution of 8 km is more likely to contain an integrated signal as well as noise. Our results indicate a relatively better performance of the MODIS NDVI model compared to the GIMMS3g NDVI model, and this is in line with the findings of Kern et al. [54]. In their comparative study of GIMMS3g and MODIS NDVI, a significant disagreement is reported and a limited

applicability of GIMMS3g is concluded for Central Europe. Moreover, GIMMS3g-based SOS and EOS detection showed poorer performance than MODIS with differences of up to 20–30 days in the majority of the cases without any systematic fashion. Amongst NDVI phenological metrics, we found that the RWI was best reflected by the summer NDVIs of current and previous years. This is in agreement with the findings of Kauffman et al. [15], who suggested that tree-rings are correlated with NDVI in the months of June–July. Other important NDVI parameters found in our study were the spring and growing season NDVIs of previous and current years. They had a higher score than precipitation in the RF model, which demonstrates the potential of NDVI metrics derived from phenology to improve RWI-climate relationships. Amongst the climatic parameters and auxiliary factors, it was precipitation, drought index scPDSI, and latitude that were highly ranked in the RF approach, whereas climate zone and tree type were the least important ones. It is worth noting that according to the variable score, summer and spring NDVIs of the previous year had a higher score than precipitation. Although scPDSI integrates the precipitation signal, the variable score reflects the potential of NDVI metrics to refine existing climate-RWI relationships. Similar results of the RF MODIS models were obtained using SPEI, a multiscalar index that takes into account the sensitivity to the evaporative demand of the atmosphere (Supplementary, Figure S5). However, the proportion of variance explained was lower (22.1% instead of 37.2%) and therefore the results were not presented in detail.

The results of our study were consistent across tree-ring chronologies set up with three different detrending methods (not shown in this paper). This clearly demonstrates that our obtained results are not an artifact of the detrending and standardization methods. Despite the considerable model improvement through the incorporation of MODIS phenological metrics, we have to stress that according to different validation metrics (Section S3, Supplementary), the RF model is still not very robust for prediction. However, with this study we aim to only compare the two NDVI datasets, to propose which NDVI phenological metrics have higher potential to explain RWI but not to reconstruct or predict RWI. One possible reason that the prediction skills are not robust could be that the present study is constrained by the assumption that the forests being analyzed lie within the NDVI pixel, which cannot be further investigated because of a lack of auxiliary information about the sites. There is no accurate information on whether species composition was homogeneous or heterogeneous across the landscape, or whether the proportions of multiple dominant species are comparable and responding similarly to climatic variables. Hence, the interpretation of NDVI and its relation to ring-widths becomes challenging. Also, tree-ring data collected originally for dendrochronological studies, if not spatially representative of a large area, can hamper correlations between the NDVI and the tree-ring data [55].

## 5. Conclusions

This paper presents the first comparison of RWI with several phenological parameters of satellite-derived proxies of vegetation activity at multiple sites in the Northern Hemisphere. We demonstrated positive associations between RWI and NDVI and between RWI and the NDVIs of preceding years, and noted that such relationships vary over space and between tree types (deciduous versus coniferous), bioclimatic zones, cumulative NDVI periods and the spatial resolution. Summer and spring NDVIs were found to be the most important NDVI metrics amongst those tested. There is strong potential for NDVI phenological metrics to improve RWI-climate relationships, especially for high-spatial-resolution NDVI, such as MODIS. However, further research is needed to investigate the robustness of the NDVI–RWI relationship. Therefore, it will be particularly interesting to see the results when more tree-ring data and longer temporal records of the high-spatial-resolution NDVI become available.

**Supplementary Materials:** The following items are available online at www.mdpi.com/2072-4292/9/6/526/s1. Figure S1: Figure showing preprocessing and phenology extraction from NDVI time series. Figure S2: Variance of Pearson correlation coefficients between time series of RWI and cumulative NDVI at different temporal scales. Section S3: Validation statistics to access performance of RF model Figure S4 Scatterplot of observed and predicted RWI. Figure S5 Random-forest variable-importance plot for RF (MODIS) climate-NDVI model

performed with drought index SPEI. Table S1: Information on sites analyzed: country, co-ordinates, species, climate zone (see climate data), elevation, important tree-ring metrics and chronology coverage.

**Acknowledgments:** The first author was supported by Deutsche Forschungsgemeinschaft (DFG) through the TUM International Graduate School of Science and Engineering (IGSSE). This research has received funding from the European Research Council under the European Union's Seventh Framework Programme (FP7/2007–2013)/ERC grant agreement no. (282250). It was performed with the support of the Technische Universität München–Institute for Advanced Study, funded by the German Excellence Initiative. The first author would like to thank Gourav Misra, Tobias Erhardt, Natalia Martín-Hernández and Fergus Reig Gracia for their input. We thank the reviewers for their contribution to the manuscript.

**Author Contributions:** Upasana Bhuyan, Annette Menzel, Sergio M. Vicente-Serrano and Christian Zang conceptualized the design of the study. Upasana Bhuyan carried out the data processing. Upasana Bhuyan and Annette Menzel wrote the manuscript. All authors contributed to the interpretation of results and editing of the manuscript.

**Conflicts of Interest:** The authors declare no conflict of interest.

## References

1. Pettorelli, N.; Vik, J.O.; Mysterud, A.; Gaillard, J.M.; Tucker, C.J.; Stenseth, N.C. Using the satellite-derived NDVI to assess ecological responses to environmental change. *Trends Ecol. Evol.* **2005**, *20*, 503–510. [CrossRef] [PubMed]
2. Danby, R.K. Monitoring forest-tundra ecotones at multiple scales. *Geogr. Compass* **2011**, *5*, 623–640. [CrossRef]
3. Biondi, F. Comparing tree-ring chronologies and repeated timber inventories as forest monitoring tools. *Ecol. Appl.* **1999**, *9*, 216–227. [CrossRef]
4. Bunn, A.G.; Hughes, M.K.; Kirdyanov, A.V.; Losleben, M.; Shishov, V.V.; Berner, L.T.; Oltchev, A.; Vaganov, E.A. Comparing forest measurements from tree rings and a space-based index of vegetation activity in Siberia. *Environ. Res. Lett.* **2013**, *8*. [CrossRef]
5. Fritts, H.C.; Blasing, T.J.; Hayden, B.P.; Kutzbach, J.E. Multivariate techniques for specifying tree-growth and climate relationships and for reconstructing anomalies in paleoclimate. *J. Appl. Meteorol.* **1971**, *10*, 845–864. [CrossRef]
6. Dobbertin, M. Tree growth as indicator of tree vitality and of tree reaction to environmental stress: A review. *Eur. J. For. Res.* **2005**, *24*, 319–333. [CrossRef]
7. Vicente-Serrano, S.M.; Camarero, J.J.; Olano, J.M.; Martín-Hernández, N.; Peña-Gallardo, M.; Tomás-Burguera, M.; Gazol, A.; Azorin-Molina, C.; Bhuyan, U.; Kenawy, A. Diverse relationships between forest growth and the Normalized Difference Vegetation Index at a global scale. *Remote Sens. Environ.* **2016**, *187*, 14–29. [CrossRef]
8. Camarero, J.J.; Franquesa, M.; Sangüesa-Barreda, G. Timing of drought triggers distinct growth responses in holm oak: implications to predict warming-induced forest defoliation and growth decline. *Forests* **2015**, *6*, 1576–1597. [CrossRef]
9. Cook, E.R.; Kairiukstis, L.A. *Methods of Dendrochronology: Applications in the Environmental Sciences*; Springer Netherlands: Dordrecht, The Netherlands, 1990.
10. Tucker, C.J. Red and photographic infrared linear combinations for monitoring vegetation. *Remote Sens. Environ.* **1979**, *8*, 127–150. [CrossRef]
11. Myneni, R.B.; Keeling, C.D.; Tucker, C.J.; Asrar, G.; Nemani, R.R. Increased plant growth in the northern high latitudes from 1981 to 1991. *Nature* **1997**, *386*, 698–702. [CrossRef]
12. Liang, E.Y.; Shao, X.M.; He, J.C. Relationships between tree growth and NDVI of grassland in the semi-arid grassland of north China. *Int. J. Remote Sens.* **2005**, *26*, 2901–2908. [CrossRef]
13. Wang, J.; Rich, P.M.; Price, K.P.; Kettle, W.D. Relations between NDVI, grassland production, and crop yield in the central Great Plains. *Geocarto Int.* **2005**, *20*, 5–11. [CrossRef]
14. Lopatin, E.; Kolström, T.; Spiecker, H. Determination of forest growth trends in Komi Republic (northwestern Russia): Combination of tree-ring analysis and remote sensing data. *Boreal Environ. Res.* **2006**, *11*, 341–353.
15. Kaufmann, R.K.; D'Arrigo, R.D.; Paletta, L.F.; Tian, H.Q.; Jolly, W.M.; Myneni, R.B. Identifying climatic controls on ring width: The timing of correlations between tree rings and NDVI. *Earth Interact.* **2008**, *12*, 1–14. [CrossRef]

16. Prince, S.D.; Tucker, C.J. Satellite remote sensing of rangelands in Botswana II. NOAA AVHRR and herbaceous vegetation. *Int. J. Remote Sens.* **1986**, *7*, 1555–1570. [CrossRef]
17. Sellers, P.J.; Randall, D.A.; Collatz, G.J.; Berry, J.A.; Field, C.B.; Dazlich, D.A.; Zhang, C.; Collelo, G.D.; Bounoua, L. A revised land surface parameterization (SiB2) for atmospheric GCMs. Part I: Model formulation. *J. Clim.* **1996**, *9*, 676–705. [CrossRef]
18. Menzel, A.; Fabian, P. Growing season extended in Europe. *Nature* **1999**, *397*. [CrossRef]
19. Menzel, A.; Sparks, T.H.; Estrella, N.; Koch, E.; Aasa, A.; Ahas, R.; Alm-Kübler, K.; Bissolli, P.; Braslavská, O.; Briede, A.; et al. European phenological response to climate change matches the warming pattern. *Glob. Chang. Biol.* **2006**, *12*, 1969–1976. [CrossRef]
20. Justice, C.O.; Townshend, J.R.G.; Holben, B.N.; Tucker, C.J. Analysis of the phenology of global vegetation using meteorological satellite data. *Int. J. Remote Sens.* **1985**, *6*, 1271–1318. [CrossRef]
21. Beck, P.S.A.; Andreu-Hayles, L.; D'Arrigo, R.D.; Anchukaitis, K.J.; Tucker, C.J.; Pinzón, J.E.; Goetz, S.J. A large-scale coherent signal of canopy status in maximum latewood density of tree rings at arctic treeline in North America. *Glob. Planet. Chang.* **2013**, *100*, 109–118. [CrossRef]
22. Berner, L.T.; Beck, P.S.A.; Bunn, A.G.; Goetz, S.J. Plant response to climate change along the forest-tundra ecotone in northeastern Siberia. *Glob. Chang. Biol.* **2013**, *19*, 3449–3462. [CrossRef] [PubMed]
23. Churkina, G.; Schimel, D.; Braswell, B.H.; Xiao, X. Spatial analysis of growing season length control over net ecosystem exchange. *Glob. Chang. Biol.* **2005**, *11*, 1777–1787. [CrossRef]
24. Richardson, A.D.; Raswell, B.H.; Hollinger, D.Y.; Jenkins, J.P. Near-surface remote sensing of spatial and temporal variation. *Ecol. Appl.* **2009**, *19*, 1417–1428. [CrossRef] [PubMed]
25. Liu, Y.; Wu, C.; Peng, D.; Xu, S.; Gonsamo, A.; Jassal, R.S.; Arain, M.A.; Lu, L.; Fang, B.; Chen, J.M. Improved modeling of land surface phenology using MODIS land surface reflectance and temperature at evergreen needleleaf forests of central North America. *Remote Sens. Environ.* **2016**, *176*, 152–162. [CrossRef]
26. Ganguly, S.; Friedl, M.A.; Tan, B.; Zhang, X.; Verma, M. Land surface phenology from MODIS: Characterization of the Collection 5 global land cover dynamics product. *Remote Sens. Environ.* **2010**, *114*, 1805–1816. [CrossRef]
27. Dong, T.; Liu, J.; Shang, J.; Qian, B.; Huffman, T.; Zhang, Y.; Champagne, C.; Daneshfar, B. Assessing the impact of climate variability on cropland productivity in the Canadian prairies using time series MODIS FAPAR. *Remote Sens.* **2016**, *8*. [CrossRef]
28. Briffa, K.R.; Osborn, T.J.; Schweingruber, F.H.; Jones, P.D.; Shiyatov, S.G.; Vaganov, E. Tree-ring width and density data around the Northern Hemisphere: Part 1, local and regional climate signals. *Holocene* **2002**, *12*, 737–757. [CrossRef]
29. MOD13Q1: MODIS/Terra Vegetation Indices 16-Day L3 Global 250m Grid SIN V006. Available online: https://lpdaac.usgs.gov/dataset_discovery/modis/modis_products_table/mod13q1_v006 (accessed on 18 February 2016).
30. GIMMS NDVI3g Dataset. ECOCAST. Available online: https://ecocast.arc.nasa.gov/data/pub/gimms/ (accessed on 26 February 2016).
31. Tree Ring. National Centers for Environmental Information, NOAA. Available online: https://www.ncdc.noaa.gov/data-access/paleoclimatology-data/datasets/tree-ring (accessed on 4 February 2016).
32. Grissino-Mayer, H.D.; Fritts, H.C. The international tree-ring data bank: An enhanced global database serving the global scientific community. *Holocene* **1997**, *7*, 235–238. [CrossRef]
33. Olivier, A.; Jose Julio, R.P.; Vasileios, K.; Bontemps, S.; Defourny, P.; Van Bogaert, E. Global Land Cover Map for 2009 (GlobCover 2009). Available online: https://doi.pangaea.de/10.1594/PANGAEA.787668 (accessed on 30 May 2016).
34. Cook, E.R.; Peters, K. Calculating unbiased tree-ring indices for the study of climatic and environmental change. *Holocene* **1997**, *7*, 361–370. [CrossRef]
35. Harris, I.; Jones, P.D.; Osborn, T.J.; Lister, D.H. Updated high-resolution grids of monthly climatic observations—The CRU TS3.10 Dataset. *Int. J. Climatol.* **2014**, *34*, 623–642. [CrossRef]
36. Jones, P. D.; Harris, I. CRU TS3.21: Climatic Research Unit (CRU) Time-Series (TS) Version 3.21 of High Resolution Gridded Data of Month-by-Month Variation in Climate (January 1901–December 2012). 2013. Available online: http://catalogue.ceda.ac.uk/uuid/ac4ecbd554d0dd52a9b575d9666dc42d (accessed on 10 Jan 2016).
37. Wells, N.; Goddard, S.; Hayes, M.J. A self-calibrating palmer drought severity index. *J. Clim.* **2004**, *17*, 2335–2351. [CrossRef]

38. CRU scPDSI 3.25. KNMI Climate Explorer. Available online: https://climexp.knmi.nl/select.cgi?id=someone@somewhere&field=scpdsi (accessed on 10 January 2016).
39. Vicente-Serrano, S.M.; Beguería, S.; López-Moreno, J.I. A multiscalar drought index sensitive to global warming: The standardized precipitation evapotranspiration index. *J. Clim.* **2010**, *23*, 1696–1718. [CrossRef]
40. Kottek, M.; Grieser, J.; Beck, C.; Rudolf, B.; Rubel, F. World map of the Köppen-Geiger climate classification updated. *Meteorol. Z.* **2006**, *15*, 259–263. [CrossRef]
41. Pinzon, J.E.; Tucker, C.J. A non-stationary 1981–2012 AVHRR NDVI3g time series. *Remote Sens.* **2014**, *6*, 6929–6960. [CrossRef]
42. Haddad, R.A.; Akansu, A.N. A class of fast Gaussian binomial filters for speech and image processing. *IEEE Trans. Signal Process.* **1991**, *39*, 723–727. [CrossRef]
43. Misra, G.; Buras, A.; Menzel, A. Effects of different methods on the comparison between land surface and ground phenology—A methodological case study from south-western Germany. *Remote Sens.* **2016**, *8*. [CrossRef]
44. Wohlfart, C.; Liu, G.; Huang, C.; Kuenzer, C. A river basin over the course of time: multi-temporal analyses of land surface dynamics in the yellow river basin (China) based on medium resolution remote sensing data. *Remote Sens.* **2016**, *8*. [CrossRef]
45. Breiman, L. Random forests. *Mach. Learn.* **2001**, *45*, 5–32. [CrossRef]
46. Rodriguez-Galiano, V.F.; Dash, J.; Atkinson, P.M. Intercomparison of satellite sensor land surface phenology and ground phenology in Europe. *Geophys. Res. Lett.* **2015**, *42*, 2253–2260. [CrossRef]
47. Pourtaghi, Z.S.; Pourghasemi, H.R.; Aretano, R.; Semeraro, T. Investigation of general indicators influencing on forest fire and its susceptibility modeling using different data mining techniques. *Ecol. Indic.* **2016**, *64*, 72–84. [CrossRef]
48. R Core Team. R: A Language and Environment for Statistical Computing. Available online: http://www.gbif.org/resource/81287 (accessed on 22 February 2017).
49. Liaw, A.; Wiener, M. Classification and regression by randomForest. *R News* **2002**, *3*, 18–22.
50. Kaufmann, R.K.; D'Arrigo, R.D.; Laskowski, C.; Myneni, R.B.; Zhou, L.; Davi, N.K. The effect of growing season and summer greenness on northern forests. *Geophys. Res. Lett.* **2004**, *31*, 3–6. [CrossRef]
51. Brehaut, L.D. 2015. The Use of NDVI and Tree Ring-Widths to Evaluate Changes in Vegetation Production in a Mountainous Boreal Landscape. Master's Thesis, Queen's University, Kingston, ON, Canada, 2015.
52. Beck, P.S.A.; Goetz, S.J. Satellite observations of high northern latitude vegetation productivity changes between 1982 and 2008: Ecological variability and regional differences. *Environ. Res. Lett.* **2011**, *6*. [CrossRef]
53. Wilmking, M.; D'Arrigo, R.D.; Jacoby, G.C.; Juday, G.P. Increased temperature sensitivity and divergent growth trends in circumpolar boreal forests. *Geophys. Res. Lett.* **2005**, *32*, 2–5. [CrossRef]
54. Kern, A.; Marjanović, H.; Barcza, Z. Evaluation of the quality of NDVI3g dataset against collection 6 MODIS NDVI in central Europe between 2000 and 2013. *Remote Sens.* **2016**, *8*. [CrossRef]
55. D'Arrigo, R.D.; Malmstrom, C.M.; Jacoby, G.C.; Los, S.O.; Bunker, D.E. Correlation between maximum latewood density of annual tree rings and NDVI based estimates of forest productivity. *Int. J. Remote Sens.* **2000**, *21*, 2329–2336. [CrossRef]